Asian Journal of Chemistry; Vol. 25, Supplementary Issue (2013), S397-S401

ASIAN JOURNAL OF CHEMISTRY

www.asianjournalofchemistry.co.in

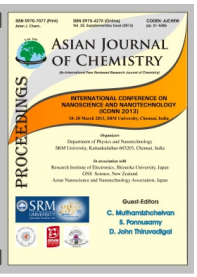

Development and Characterization of Lithium Manganese Oxide Thinfilms for Li ion Micro Battery Application†

N. SANKARA SUBARAMANIAN* and T. BALAKRISHNAN

Thinfilm Research Laboratory, Department of Physics, Thiagarajar College of Engineering, Madurai-625 015, India

*Corresponding author: E-mail: shankersathiya@yahoo.com

AJC-12886

$LiMn_2O_4$ thin films have been prepared by cost-effective spin coating method using the optimized coating conditions. The X-ray diffraction pattern of $LiMn_2O_4$ thin films confirms cubic spinel structure with the preferred orientation along the (111) plane. The other orientations observed correspond to (311), (400) and (440) plane. The sharpness and peak intensity of all the above prominent orientations increase with the increase in the number of coatings and spin rate. This may be attributed to the increase in degree of crystallinity, oriented growth of all the planes and densification of crystallite aggregates with the increase in number of coatings and spin rate. The lattice constant 'a' evaluated from the XRD data lies between 8.11619 and 8.13482 A°. The mean grain size increases with the increase in the number of coatings and this may be attributed to the increase in the accumulation and adhesion of the crystallites on the substrate surface with the increase in the number of coatings. The micro strain and dislocation density of the $LiMn_2O_4$ thin films increases with the increase in the number of coatings and this may be ascribed to the increase in the close packing of crystallite aggregates, which ultimately increases the thermal and mechanical shock resistance to the substrate surface. The FTIR spectra of $LiMn_2O_4$ thin films deposited with different spin rate and number of coatings illustrates the high-frequency bands located around 623 cm^{-1} and 514 cm^{-1} and these are associated with the asymmetric stretching modes of the MnO_6 group. A weak band observed at 437 cm^{-1} is attributed to the LiO_4 tetrahedra. The AFM micrographs of the $LiMn_2O_4$ thinfilms deposited at 3000 rpm shows the uniform distribution of fine grains throughout the surface associated with the accumulation of fine grains without any dark pits, pin holes and cracks.

Key Words: Thin film micro battery, $LiMn_2O_4$ thin films, Spinel structure, Mean grain size, Micro strain, Dislocation density.

INTRODUCTION

Spinel lithium manganese oxide ($LiMn_2O_4$) has been extensively studied as the most promising cathode material for lithium-ion batteries, since it is low cost, environmentally benign, has fast charging-discharging characteristics, good thermal behaviour, which does not require additional expensive safety device and non toxicity as compared to layered oxides such as $LiCoO_2$ and $LiNiO_2$[1,2]. Now-a-days $LiMn_2O_4$ thin films have been fabricated by a variety of methods such as radio frequency magnetron sputtering[3,4], electrostatic spray deposition[5,6], sol-gel spin coating technique[7-13,15-17], ultrasonic spray deposition[14] and so on. The $LiMn_2O_4$ thin films prepared by various methods differ much from their properties, which is mainly due to the synthesizing procedures. The sol gel spin coating method is an alternative procedure for the deposition of thin film $LiMn_2O_4$ cathodes owing to its simple, economical and easy process. It has been well demonstrated that the sol-gel process offers good mixture of the starting materials. However, quality of the deposited thinfilms is highly dependent on the nature of precursor solution and the prime requirements of the precursor solution are higher order of homogeneity, chemical stability and adherence to substrate surface. The structure of cubic spinel $LiMn_2O_4$ (space group: Fd3m) involves a cubic close packed oxygen array, with octahedrally coordinated Mn ions in the 16d site and tetrahedrally coordinated Li ions in the 8a site. Li ions are extracted from the structure on charging and reinserted on discharging[18,19]. This material is known to show capacity fading on cycling, which may be caused in part by structural changes which have been studied extensively using different techniques *viz*., X-ray diffraction, atomic force microscopy, infrared absorption and theoretical calculations. The present work deals with the development of $LiMn_2O_4$ thin films by the sol-gel spin coating method using the optimized coating parameters and to investigate the influence of spin rate and number of coatings on its structural, optical and surface properties.

EXPERIMENTAL

The sol solution have been prepared by mixing alcoholic solutions of 2 M lithium acetate ($CH_3COOLi{\cdot}2H_2O$) and 2 M

†International Conference on Nanoscience & Nanotechnology, (ICONN 2013), 18-20 March 2013, SRM University, Kattankulathur, Chennai, India

manganese nitrate [$Mn(NO_3)_2 \cdot 4H_2O$] dissolved in appropriate amount of ethyl alcohol. The mixed solutions have been refluxed at 60 ºC for 1 h, air cooled and then allowed for ageing. Lithium manganese oxide thin films have been spin coated on mineral glass substrate. The following optimized process parameters have been used for coating the $LiMn_2O_4$ thin films: Spin time-10 Sec, heat treatment temperature -400 ºC and heat treatment duration-5 min. In order to evaluate the influence of spin rate and number of coatings on the properties of the $LiMn_2O_4$ films, in the present work $LiMn_2O_4$ thinfilms have been deposited on glass substrate with different spin rate *viz.*, 2000, 2500, 3000, 3500 and 4000 RPM and different number of coatings *viz.*, 2, 4, 6, 8, 10 and 12 respectively. The developed $LiMn_2O_4$ thin films have been annealed at 400 ºC in an atmospheric furnace for 1 h. Structural properties of the as deposited films have been studied using the philips Pan-analytical X-ray diffractometer. From the measured XRD data crystallographic properties *viz.*, lattice constant, mean grain size, micro strain and dislocation density of the $LiMn_2O_4$ thinfilms have been evaluated. Configuration of molecular spices and changes in the coordination of the compound has been studied using the SHIMADZU Fourier-transform infrared spectrophotometer. Surface features of the $LiMn_2O_4$ thinfilms have been analyzed using the 2D and 3D AFM images recorded in an atomic force microscope.

RESULTS AND DISCUSSION

Structural characterization: The X-ray diffraction pattern of $LiMn_2O_4$ thin films deposited with different number of coating and spin rate are shown in Figs. 1 and 2. The diffraction peaks of all the samples have been identified as cubic spinel structure with the space group Fd3m in which the lithium ions occupy the tetrahedral (8a) sites and manganese reside at the octahedral (16d) sites with preferred orientation along the (111) plane[18,19]. The other orientations observed in the XRD profiles correspond to (311), (400) and (440) plane. The sharpness and peak intensity of all the above prominent orientations increases with the increase in the number of coatings and spin rate[7-11]. This may be attributed to the increase in degree of crystallinity and densification of crystallite aggregates with the increase in number of coatings and spin rate. The growth of an additional orientation (422) plane has been observed for the $LiMn_2O_4$ thinfilm spin coated above 6 numbers of coatings and sharpness, peak intensity of this plane gradually increases upto 12 numbers of coating[15-17]. This may be attributed to the excessive oriented over growth of crystallites due to the rise in the accumulated particles with the increase in the number of coatings. The crystallographic parameters *viz.*, lattice constant mean grain size, micro strain and dislocation density of $LiMn_2O_4$ thinfilms spin coated with different number of coatings and spin rate have been evaluated from the XRD data and is shown in the Tables 1 and 2, respectively.

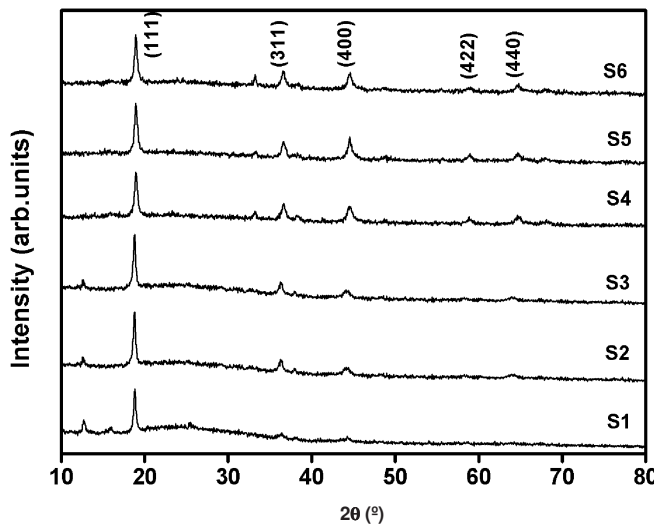

Fig. 1. XRD pattern of $LiMn_2O_4$ thin films spin coated with different number of coatings (S1 = 2 coat, S2 = 4 coat, S3 = 6 coat, S4 = 8 coat, S5 = 10 coat and S6 = 12 coat)

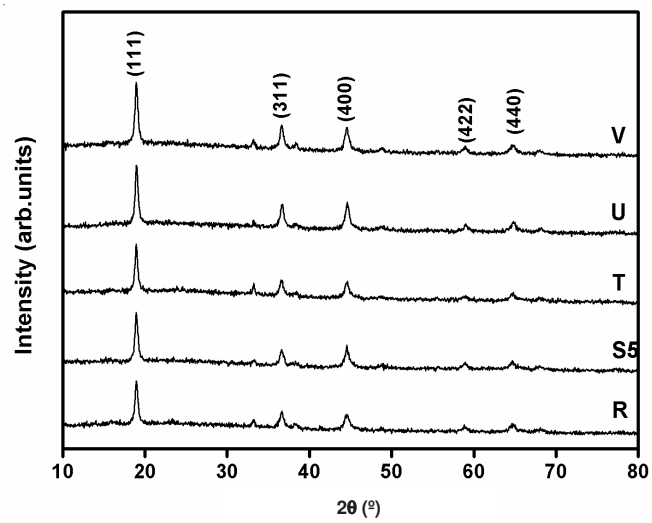

Fig. 2. XRD pattern of $LiMn_2O_4$ thin films spin coated at different spin rate (R = 2000 rpm, S5 = 2500 rpm, T = 3000 rpm, U = 3500 rpm and V = 4000 rpm)

TABLE-1
VARIOUS CRYSTALLINE PARAMETERS EVALUATED FROM THE XRD DATA OF THE $LiMn_2O_4$ THIN FILMS SPIN COATED WITH DIFFERENT NUMBER OF COATINGS

Number of coatings	Mean grain size (D) (nm)	Micro strain (ε) $\times 10^{-3}$	Dislocation density (δ) $\times 10^{15}$ (line/m^2)	Lattice constant (a) (Å)
12	16.81513	2.1089	3.77994	8.13166
10	7.56602	0.50905	0.64699	8.12727
8	19.13962	1.84710	2.90004	8.12705
6	19.5722	1.90528	3.25389	8.12689
4	2.64813	1.45441	5.28141	8.12643
2	66.20400	0.81447	0.70560	8.12567

TABLE-2
VARIOUS CRYSTALLINE PARAMETERS EVALUATED FROM THE XRD DATA OF THE $LiMn_2O_4$ THIN FILMS DEPOSITED AT DIFFERENT SPIN RATE

Number of coatings	Mean grain size (D) (nm)	Micro strain (ε) $\times 10^{-3}$	Dislocation density (δ) $\times 10^{15}$ (line/m^2)	Lattice constant (a) (Å)
4000	16.49844	2.19616	4.20139	8.13482
3500	17.64580	2.00709	3.41710	8.13446
3000	17.78792	1.79255	3.37326	8.13406
2500	7.56602	0.50905	0.64699	8.12727
2000	18.04317	1.93437	3.13560	8.11619

The lattice constant 'a' evaluated from the XRD data lies between 8.11619 and 8.13482 Å, which is well in agreement with the standard JCPDS PDF data file number 89-4604. Variation of mean grain size, micro strain and dislocation density of the $LiMn_2O_4$ thinfilms deposited with different spin rate and number of coatings is shown in the Figs. 3 and 4 respectively. The mean grain size increases with the increase in the number of coatings and this may be attributed to the increase

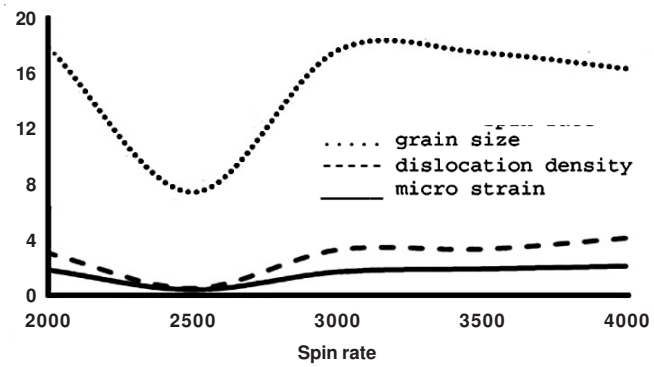

Fig. 3. Variation of mean grain size, micro strain and dislocation density of the $LiMn_2O_4$ thin films deposited at different spin rate

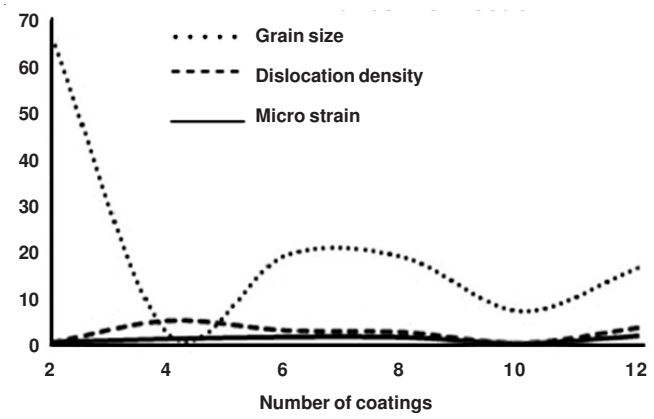

Fig. 4. Variation of mean grain size, micro strain and dislocation density of the $LiMn_2O_4$ thin films spin coated with different number of coatings

in the accumulation and adhesion of the crystallites on the substrate surface with the increase in the number of coatings, which ultimately increases the other associated parameters such as micro strain and dislocation density. All the crystallographic parameter of the $LiMn_2O_4$ thin films listed in the Table-2 are observed to increase with the rise in the spin rate. This may be ascribed to the increase in the close packing of crystallite aggregates with the spin rate, as evidenced by the marginal increase in the lattice constant. This may also be attributed to the increase in the packing of crystallites with spin rate causes an increase in the thermal and mechanical shock resistance to the film surface, which ultimately influence the increasing effect on the micro strain and dislocation density.

FTIR analysis: Vibrational modes that are attributed to the motion of cations with respect to their oxygen neighbours are sensitive to the point group symmetry of the cations in the oxygen host matrix. Hence the local environment of the cations in a lattice of close-packed oxygen can be studied by FTIR spectroscopy. The FTIR spectra of $LiMn_2O_4$ thin films spin coated with different spin rate and number of coatings is shown in the Figs. 5 and 6. The vibrational modes have been observed for all the samples around 437 cm^{-1}, 514 cm^{-1} and 623 cm^{-1}. The two higher wave number peaks could be attributed to the asymmetric stretching vibration modes of the Mn-O_6 group

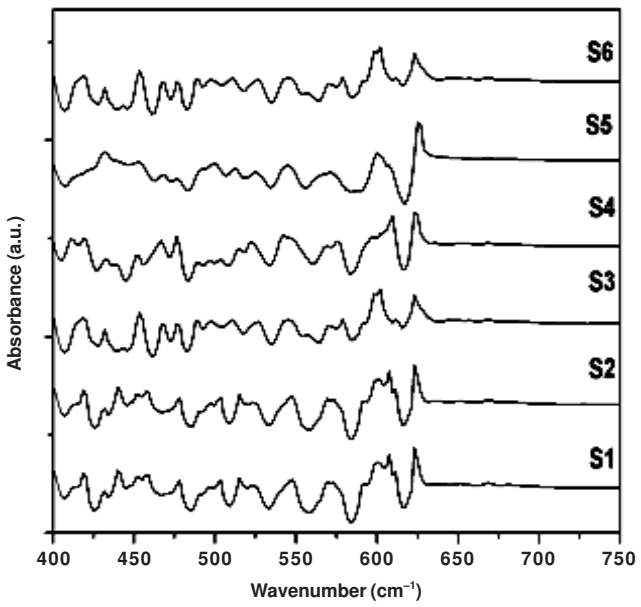

Fig. 5. FTIR spectra of $LiMn_2O_4$ thin films spin coated with different number of coatings (S1 = 2 coat, S2 = 4 coat, S3 = 6 coat, S4 = 8 coat, S5 = 10 coat and S6 = 12 coat)

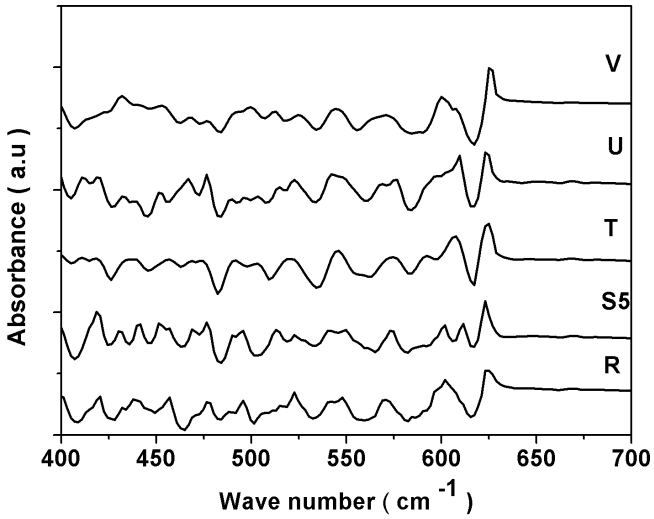

Fig. 6. FTIR spectra of $LiMn_2O_4$ thin films deposited at different spin rate (R = 2000 rpm, S5 = 2500 rpm, T = 3000 rpm, U = 3500 rpm and V = 4000 rpm)

and the lower wavenumber peak corresponds to tetrahedral stretching vibration of Li-O_4 group and these results are well in agreement with the reported results[20].

Surface characterization: As the physical and structural characteristics of the $LiMn_2O_4$ thinfilm spin coated with 12 numbers of coating and at the spin rate 3000 rpm is observed to be higher, in this work the AFM surface investigation have been carried out for these specimen. The 2D and 3D AFM image of the $LiMn_2O_4$ thinfilms spin coated with 12 numbers

of coating and the spin rate 3000 rpm is shown in the Figs. 7-10 respectively. The AFM micrographs of the $LiMn_2O_4$ thinfilms spin coated with 12 numbers of coatings clearly

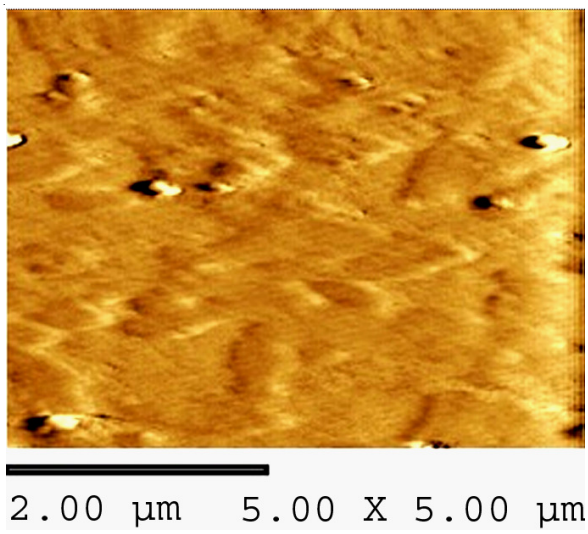

Fig. 7. 2D AFM image of the $LiMn_2O_4$ thin film spin coated with 12 numbers of coating

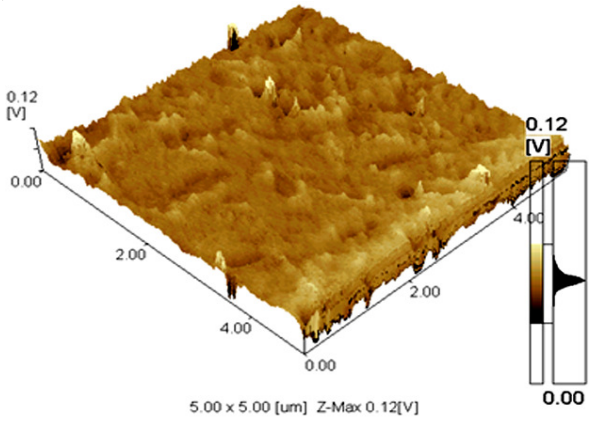

Fig. 8. 3D AFM image of the $LiMn_2O_4$ thin film spin coated w ith 12 numbers of coating

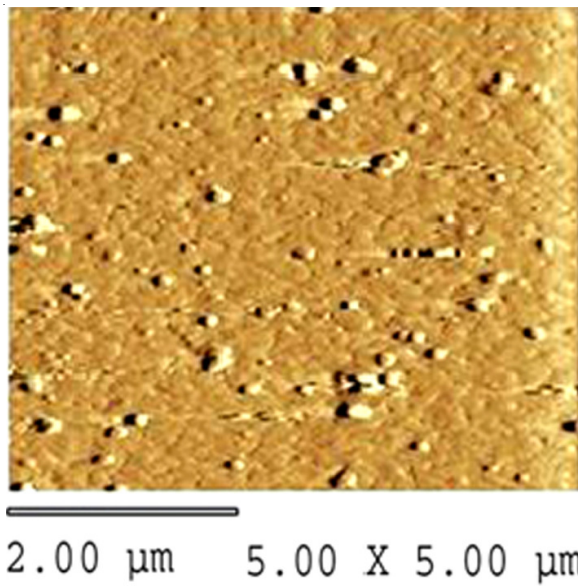

Fig. 9. 2D AFM image of the $LiMn_2O_4$ thin film deposited at 3000 rpm

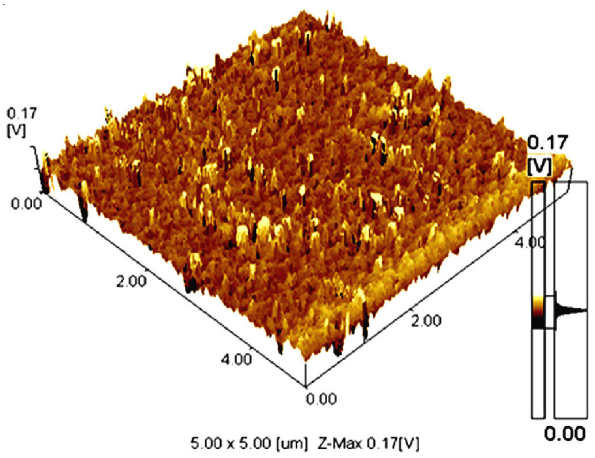

Fig. 10. 3D AFM image of the $LiMn_2O_4$ thin film deposited at 3000 rpm

indicate an uniform surface pattern, with the large crystallites and the presence of unevenly distributed coarse grains and small valley. The $LiMn_2O_4$ thinfilm spin coated at 3000 rpm illustrates the uniform distribution of fine grains throughout the surface associated with the accumulation of fine grains without any dark pits, pin holes and cracks.

Conclusion

$LiMn_2O_4$ thin films have been prepared by cost effective spin coating method using the optimized coating conditions. The XRD profile of $LiMn_2O_4$ thinfilms confirms cubic spinel structure with the preferred orientation along the (111) plane. The sharpness and peak intensity of all the prominent orientations increases with the increase in the number of coatings and spin rate. This may be attributed to the increase in degree of crystallinity and densification of crystallite aggregates with the increase in number of coatings and spin rate. The growth of an additional orientation along the (422) plane has been observed for the $LiMn_2O_4$ thin film spin coated above 6 numbers of coatings and sharpness, peak intensity of this plane gradually increases upto 12 numbers of coatings. This may be attributed to the excessive oriented over growth of crystallites due to the rise in the accumulated particles with the increase in the number of coatings. The lattice constant a evaluated from the XRD data lies between 8.11619 and 8.13482 Å, which is well in agreement with the standard JCPDS PDF data file number 89-4604. The mean grain size increases with the increase in the number of coatings and this may be attributed to the increase in the accumulation and adhesion of the crystallites on the substrate surface with the increase in the number of coatings, which ultimately increases the other associated parameters such as micro strain and dislocation density. All the crystallographic parameters of the $LiMn_2O_4$ thin films increase gradually with the rise in spin rate. This may be ascribed to the increase in the close packing of crystallite aggregates with the spin rate. This causes an increase in the thermal and mechanical shock resistance to the film surface, which ultimately influence the increasing effect on the micro strain and dislocation density The FTIR spectra of $LiMn_2O_4$ thinfilms deposited with different spin rate and number of coatings illustrates the high-frequency bands located around the wavenumber 623 cm^{-1} and 514 cm^{-1} and these are associated

with the asymmetric stretching modes of the Mn-O_6 group. A weak band observed at the wavenumber 437 cm^{-1} is attributed to the vibrations of Li-O_4 tetrahedral. The AFM micrographs of the $LiMn_2O_4$ thinfilms spin coated with 12 numbers of coatings clearly indicate an uniform surface pattern, with the large crystallites and the presence of unevenly distributed coarse grains and small valley. The $LiMn_2O_4$ thinfilm spin coated at 3000 rpm illustrates the uniform distribution of fine grains throughout the surface associated with the accumulation of fine grains without any dark pits, pin holes and cracks.

REFERENCES

1. I. Taniguchi, N. Fukuda and M. Konarova, *Powder Technol*., **181**, 228 (2008).
2. L. Yang, M. Takahashi and B.F. Wang, *Electrochim. Acta*, **51**, 3228 (2006).
3. C.C. Chen, K.-F. Chiu, K.M. Lin and H.C. Lin, *Thin Solid Films*, **517**, 4192 (2009).
4. H.-S. Moon, W.H. Lee, P.J. Reucroft and J.-W. Park, *J. Power Sour*., **119-121**, 710 (2003).
5. T. Doi, T. Yahiro, S. Okada and J.-i. Yamaki, *Electrochim. Acta*, **53**, 8064 (2008).
6. C.H. Chen, E.M. Kelder and J. Schoonman, *J. Power Sour*., **68**, 377 (1997).
7. L. Tian and A. Yuan, *J. Power Sour*., **192**, 693 (2009).
8. C.L. Tan, Zhou, W.S. Li, X.H. Hou, D.S. Lu, M.Q. Xu and Q.M. Hung, *J. Power Sour*., **184**, 408 (2008).
9. Y.J. Park, J.G. Kim, M.K. Kim, H.T. Chung and Y. Park, *J. Power Sour*., **87**, 69 (2000).
10. S.-W. Jang, H.-Y. Lee, K.-C. Shin, S.M. Lee, J.-K. Lee, S.-J. Lee, H.-K. Baik and D.-S. Rhee, *J. Power Sour*., **88**, 274 (2000).
11. Y.-K. Sun, *Solid State Ionics*, **100**, 115 (1997).
12. A. Subramania, S.N. Karthick and N. Angayarkanni, *Thin Solid Films*, **516**, 8295 (2008).
13. Y. Iriyama, Y. Tachibana, R. Sasasoka, N. Kuwata, T. Abe, M. Inaba, A. Tasaka, K. Kikuchi, J. Kawamura and Z. Ogumi, *J. Power Sour*., **174**, 1057 (2007).
14. Y. Wang, W. Chen, Q. Luo, S. Xie and, C.H. Chen, *Appl. Surf. Sci.*, **252**, 8096 (2006).
15. H.X. Liang, X. Zhao, Z.Y. Yu, M.H. Cao and H.X. Liu, *Solid State Ionics*, **192**, 339 (2011).
16. F.-Y. Shih and K.-Z. Fung, *J. Power Sour*., **159**, 179 (2006).
17. F.-Y. Shih and K.-Z. Fung, *J. Power Sour*., **158**, 1370 (2006).
18. T. Tsuji, M. Nagao, Y. Yamamura and N.T. Tai, *Solid State Ionics*, **154-155**, 381 (2002).
19. H. Bjork, T. Gustafsson and J.O. Thomas, *Electrochemistry*, **3**, 187 (2001).
20. P. Kalyani, N. Kalaiselvi and N. Muniyandi, *J. Power Sour*., **111**, 232 (2002).